COBEM 2023 27TH INTERNATIONAL CONGRESS OF MECHANICAL ENGENEERING

ABCM Brazilian Society of Mechanical Sciences and Engineering
27th ABCM International Congress of Mechanical Engineering
December 04-08, 2023, Florianópolis-SC, Brazil

COB-2023-0122
EFFECT OF MOVING VEHICLES ON THE FLOW AND DISPERSION OF CARBON MONOXIDE IN AN URBAN CANYON

Gabriel Gusmão Almeida
Fernanda Capucho Cezana
Federal Institute of Science and Technology of Espírito Santo – *campus* São Mateus
gabrielgusmaoalmeida@hotmail.com
fecezana@ifes.edu.br

Abstract. *The urbanization has never been so present in cities and together with it comes an increase in vehicle fleet and building density present in urban zones, becoming necessary studies about the impacts that these advancements have been causing on the air quality that we breathe. This work aims to study the behavior of carbon monoxide dispersion and flow, coming from automobile emissions, inside an idealized urban canyon. The vehicle induced turbulence influence over the carbon monoxide flow and dispersion were evaluated, considering two different moving vehicle velocities. For that, the finite volume method together with a non-structured polyhedral mesh present in the numerical simulation software Ansys Fluent© 22.0 was used, in which it solved the mass, momentum and chemical species conservation equations. Beyond that, turbulence modelling was performed using the Reynolds Averaged Navier-Stokes (RANS) approach. The numerical results were compared with data obtained from wind tunnel experiments and similar numerical simulation results present in the literature. It can be verified that the variables of interest such as velocity, turbulent kinetic energy and carbon monoxide concentrations were strongly influenced by the vehicle velocity change, mainly when compared with the standing vehicle case.*

Keywords: *Computational Fluid Dynamics, Urban canyon, Carbon monoxide dispersion, Vehicle Induced Turbulence*

1. INTRODUCTION

An intense city growth and urbanization has been seen in the last years, together with the construction of buildings and skyscrapers and the continuous motivation of vehicle utilization such as cars and motorcycles, cooperating in a manner that vehicle sourced pollutants emission increases each time more. (Shi et al., 2020).

According to the World Health Organization, Almost the entire global population (99%) breathes air that exceeds WHO air quality limits, threatening their health. A record number of over 6000 cities in 117 countries are now monitoring air quality, but the people living in them are still breathing unhealthy levels of fine particulate matter and nitrogen dioxide, with people in low and middle-income countries suffering the highest exposures (WHO, 2022).

According to Zhao et al. (2021), analyzing the fluid flow turbulent behavior and the pollutant dispersion inside urban canyons is a topic that stands out in the world scientific literature, given that the pollution around and inside urban canyons become more severe due to possible structural changes such as building's width and height and the presence of vehicles and traffic.

Cai et al. (2020) comment that there are three primary major mechanisms for turbulent generation in these canyons, the wind induced turbulence (WIT), the thermal induced turbulence (TIT) and the vehicle induced turbulence (VIT), highlighting that although the first two are more researched, the VIT still has a lot of space to be explored.

Zhao et al. (2021) discuss that the three most used methodologies for considering VIT in numerical simulations are the aerodynamic relative speed method, the dynamic mesh method and the additional turbulence source term method. They affirm that the additional turbulence source term method has been confirming itself as an adequate method since it unites low computational cost and satisfactory precision.

The aim of this study is to investigate the influence of vehicle speed over the carbon monoxide concentration inside an idealized urban canyon with external air flow using the additional turbulence source term method.

2. METHODOLOGY

In the present work the air flow in an idealized street canyon was investigated using numerical simulation. Figure 1 shows the computational domain, which was defined according to the wind tunnel experiment developed by Kastner-Klein et al. (2001), with two buildings of fixed height, $H = 120$ mm. They occupy an area of 1200×120 mm² each and the Reynolds number based on the building height in the experimental conditions was $Re \approx 5.7 \cdot 10^4$ and the Schmidt's number used to predict the total diffusivity was adopted as $Sc = 0.7$.

The reference wind measured adopted was $u_0 = 7\ \mathrm{m\ s^{-1}}$. The origin of the coordinate system is in the center of the model. More details of wind tunnel experiments are described in Kastner-Klein et al. (2001).

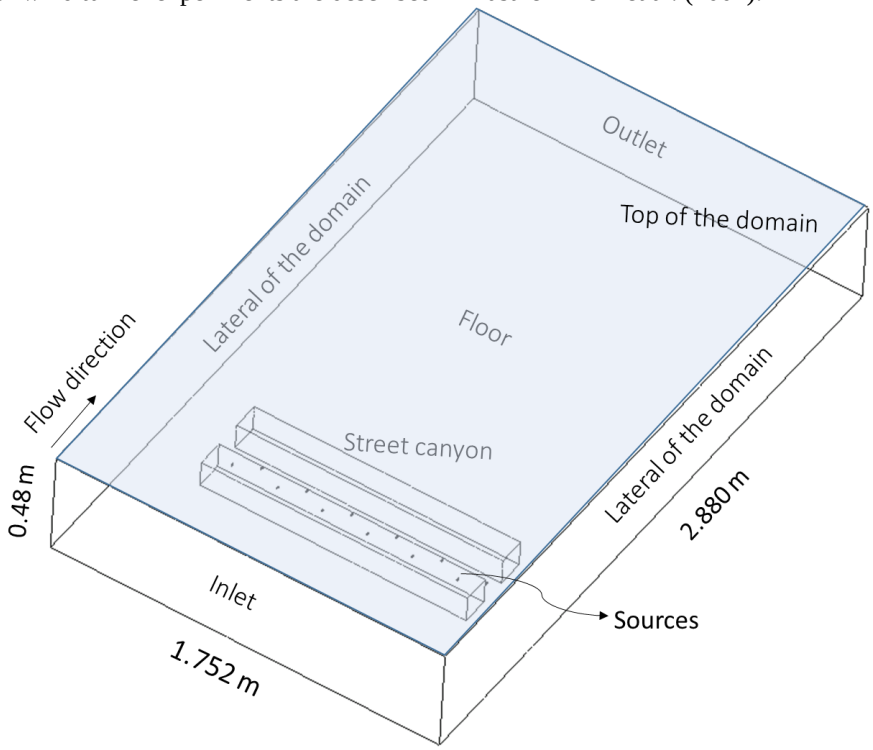

Figure 1. 3D representation of the model proposed by Solazzo et al. (2008).

2.1 Governing equations and Numerical method

The Equations 1 and 2 are used to the describe the fluid flow through the mass and momentum conservation, respectively, and Equation 3 is used to describe the carbon monoxide (CO) dispersion through an advective-diffusive transport equation. The Reynolds Averaged Navier Stokes (RANS) mean is applied in all three equations and the turbulence closure model used is the Standard k – ε model. The equations below also simplified the case by considering a neutral atmospheric state implying that there are no temperature gradients, thus, the energy conservation equation isn't solved.

$$\frac{\partial \overline{u_j}}{\partial x_j} = 0, \tag{1}$$

$$\rho \frac{\partial \overline{u_i u_j}}{\partial x_j} = -\frac{\partial \overline{p}}{\partial x_i} + g\delta_{i3} + \mu \frac{\partial^2 \overline{u_i}}{\partial x_j \partial x_j} + \frac{\partial \tau_{ij}}{\partial x_j} + F_m. \tag{2}$$

$$\rho \frac{\partial \overline{u_j c}}{\partial x_j} = D \frac{\partial^2 \overline{c_i}}{\partial x_j \partial x_j} + M. \tag{3}$$

The equations are numerically solved in steady-state regime, using the finite volume method of *Ansys Fluent*® 22.0 computational code. Aiming to show that our numerical solution does not depend on the used mesh, a mesh sensibility test was taken, but it is not shown. The same simulation conditions are tested in three levels of mesh discretization: 1.25, 2.5 and 5 million nodes, with the Standard $k - \varepsilon$ model and the Navier-Stokes equation discretized using a second-order scheme in space. The 2.5 million node mesh was chosen to conduct the study.

The additional source terms used to model the Vehicle Induced Turbulence (VIT) were implemented in the Standard k – ε model, as shown in Equations (4) to (8). (Zhao et al., 2021)

$$\rho \frac{\partial k \bar{u}_i}{\partial x_i} = \frac{\partial}{\partial x_i}\left[\left(\mu + \frac{\mu_t}{\sigma_k}\right)\frac{\partial k}{\partial x_i}\right] - \rho \bar{u}_i \bar{u}_j \frac{\partial u_j}{\partial x_i} - \rho\varepsilon + F_k, \tag{4}$$

$$\rho \frac{\partial \varepsilon \bar{u}_i}{\partial x_i} = \frac{\partial}{\partial x_i}\left[\left(\mu + \frac{\mu_t}{\sigma_\varepsilon}\right)\frac{\partial \varepsilon}{\partial x_i}\right] - C_{1\varepsilon}\rho \frac{\varepsilon}{k}\bar{u}_i \bar{u}_j \frac{\partial u_j}{\partial x_i} - C_{2\varepsilon}\rho \frac{\varepsilon^2}{k} + F_\varepsilon. \tag{5}$$

$$F_m = -\rho \frac{1}{2} C_{f-car} \frac{A_{car}}{Volume_{fluid}} (\bar{u}_i - u_{car,i}) \sqrt{(\bar{u}_j - u_{car,j})^2}, \tag{6}$$

$$F_k = (\bar{u}_i - u_{car,i}) F_m, \tag{7}$$

$$F_\varepsilon = \varepsilon \sqrt{k} \frac{C_{\varepsilon-car}}{L_{car}}. \tag{8}$$

The Standard k – ε turbulence closure model constants used are $C_\mu = 0.09$, $C_{1\varepsilon} = 1.44$, $C_{2\varepsilon} = 1.92$ (Richards and Hoxey, 1993), $\sigma_k = 0.53$ e $\sigma_\varepsilon = 0.55$ (Solazzo et al., 2007). And the source terms constants are $C_{f-carro}$ which is the car aerodynamic drag coefficient, considered equal to 0.3 (Zhao et al., 2021), A_{car} is the vehicle frontal area in the direction of its speed, which is also perpendicular to the flow direction, $Volume_{fluid}$ is the fluid volume in which the drag force acts, u_{car} is the car speed, $C_{\varepsilon-carro} = 0.025$ is the ratio between the car length L_{car} and the turbulent length scales inside the canyon.

The source term M was modelled in a manner that represented the vehicle's CO emissions effects, as shown in Equation (9). A specific cell was separated behind each vehicle, as seen in Figure 2, and only in these cells M is calculated. The volume of each cell is given by $Volume_{cell}$. The mass flow rate used was $\dot{m} = 5.52 \times 10^{-4} g/s$, based on 2019 average annual vehicle emissions of the city of São Paulo (CETESB, 2019).

$$M = \frac{\dot{m}}{Volume_{cell}}. \tag{9}$$

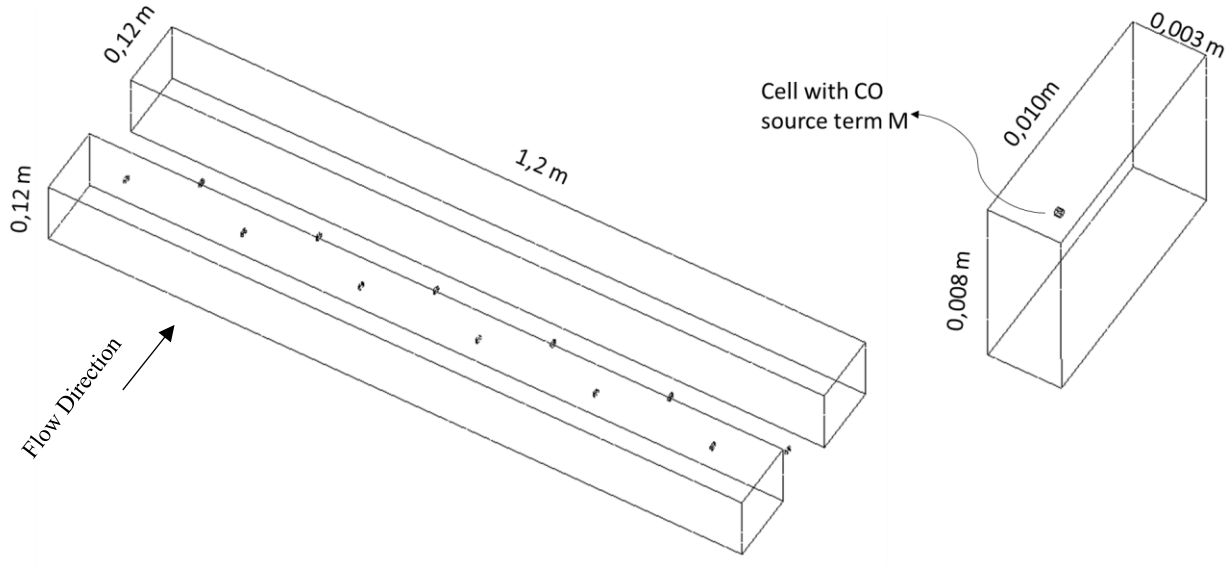

Figure 2. Dimension details of buildings and source term positioning.

2.2 Boundary conditions

Table 1 shows boundary conditions used in this study, which are the same that were used in Solazzo et al (2008), where $u_* = 0.43\ \mathrm{m}s^{-1}$, $\kappa = 0.4187$ is the Von Kárman constant, $z_o = 0.0007\ m$, $\delta = 0.48\ m$ is the boundary layer depth and $C_\mu = 0.09$ (Kastner Klein et al., 2001).

Table 1. Boundary conditions

Inlet	$u(z) = \frac{u_*}{\kappa}\ln\left(\frac{z}{z_0}+1\right)$, $k(z) = \frac{u_*^3}{\sqrt{C_\mu}}\left(1-\frac{z}{\delta}\right)$, $\varepsilon(z) = \frac{u_*^2}{\kappa(z+z_0)}\left(1-\frac{z}{\delta}\right)$, Zero CO concentration.
Outlet	Outflow
Laterals and top	Symmetry and Zero CO flux
Buildings walls and bottom	No-slip and Zero CO flux

3. RESULTS AND DISCUSSION

Data were collected and compared with wind tunnel data provided by Kastner-Klein et al. (2001) in 15 lines equally spaced by 0.05m, which are shown in Figure 3. They have a height of 2.5H and are all on the middle of the canyon between the buildings.

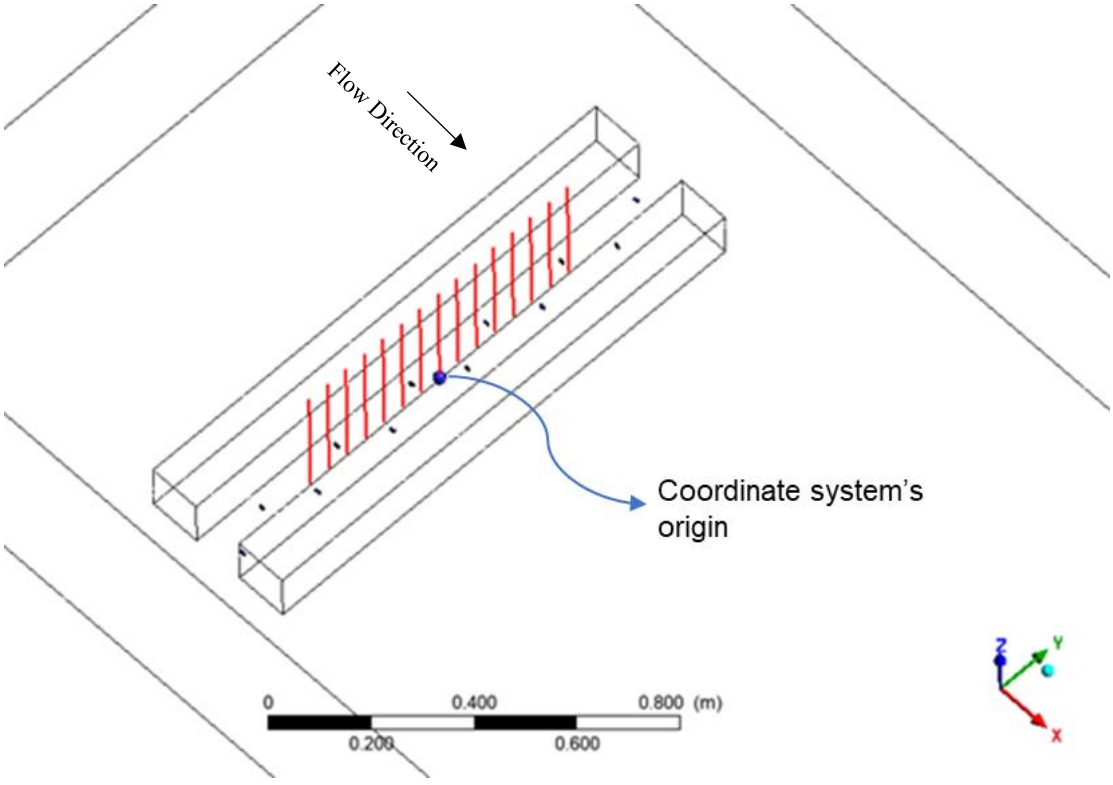

Figure 3. Positioning of the 15 lines from where the data was obtained and analyzed.

Figure 4 shows a comparison of the mean velocity vertical profile considering the Kastner-Klein et al. (2001) wind tunnel data where they considered moving vehicles, the present work case where no moving vehicles were considered and the present work case where the moving vehicles were considered with a velocity of 5 ms^{-1}, the same imposed in the wind tunnel. There's a noticeably good agreement with the wind tunnel data.

It can also be noted that, close to the floor, the turbulent kinetic energy is higher due to the moving cars and the model could predict a peak at approximately 1.2H, just as the experiment, although the values near the floor are off by a certain amount, probably due to the way that the VIT source term modelling was done.

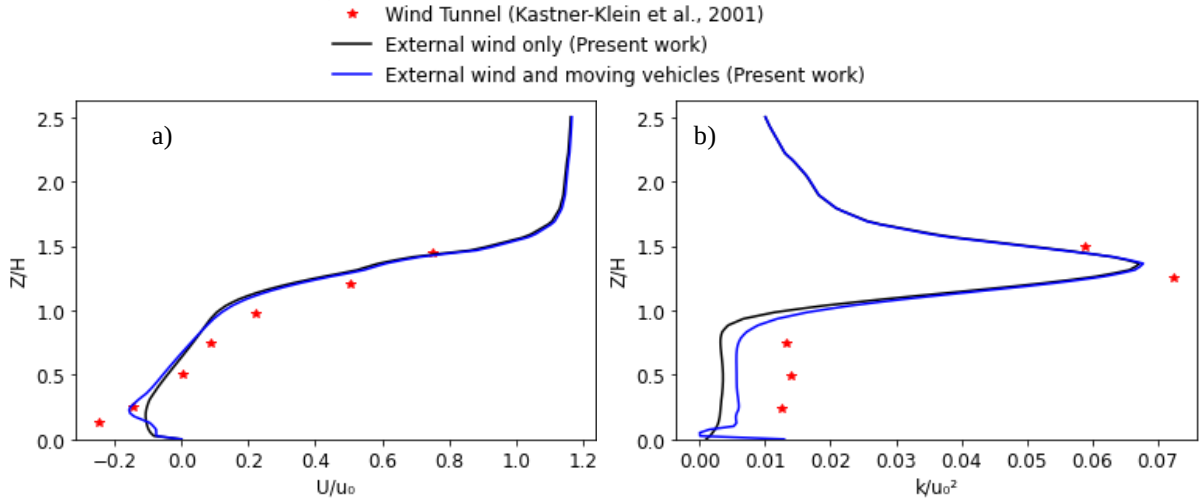

Figure 4. Vertical profiles of the 15 vertical lines average a) Mean velocity in the x direction and b) Turbulent kinetic energy.

3.1 Mean velocity fields

The shape obtained in Figure 5 matches with what is predicted in the literature (Oke, 1988), and that is determined by the ratio between the canyon's width and the buildings height, which in this case is equal to 1. The observed flow in this scenario is commonly referred to as skimming flow. It occurs due to the boundary layer separation in the building boundary at downstream, contributing to the vortex's formation in regions next to the building walls and inside the canyon.

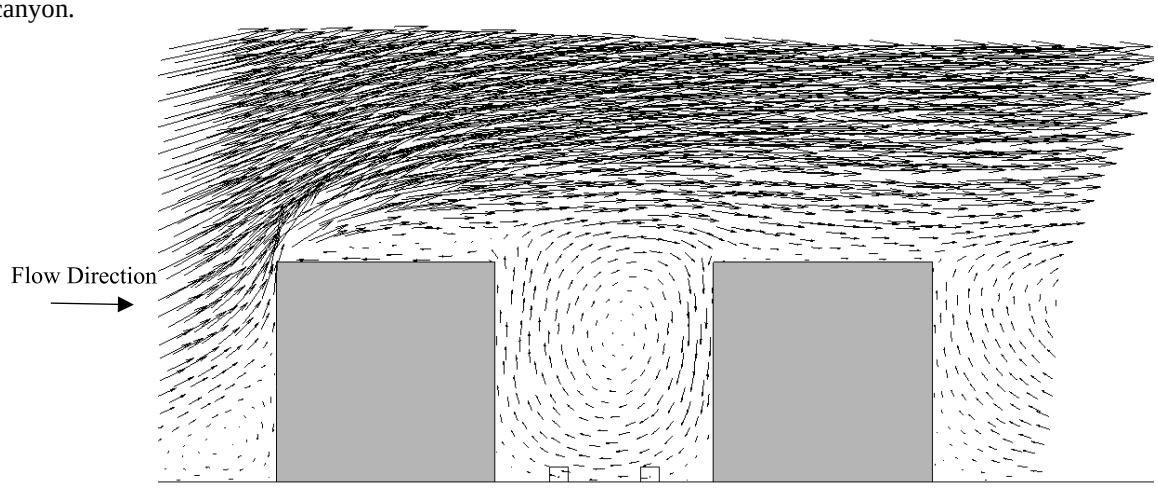

Figure 5. Mean velocity field at the Y/H = 0 plane.

Figure 6 shows that vehicle speed influence directly the flow inside the canyon, with faster velocities near the floor but with a decrease in regions far from the floor. In Figure 6b the vehicle speed was considered equal to 20kmh^{-1}. In the plane located at the vehicle's height, z/H =0.066, the mean velocity stays around 5.5 ms^{-1}, or approximately 20 kmh^{-1}. This value keeps decreasing as the height increases and it is noted that for the planes z/H = 0,5 and z/H = 1 the mean velocity distribution tends to be more homogeneous, not being too much influenced by the vehicle speed. A similar behavior is shown in Figure 6c, where the vehicle speed is 40kmh^{-1}, reducing until it reaches the open flow region. It's

worth mentioning that vehicle speed also influenced the flow in the regions above, increasing the velocity magnitude due to the vertical momentum transport. In all cases the main flow is directed perpendicular to the buildings.

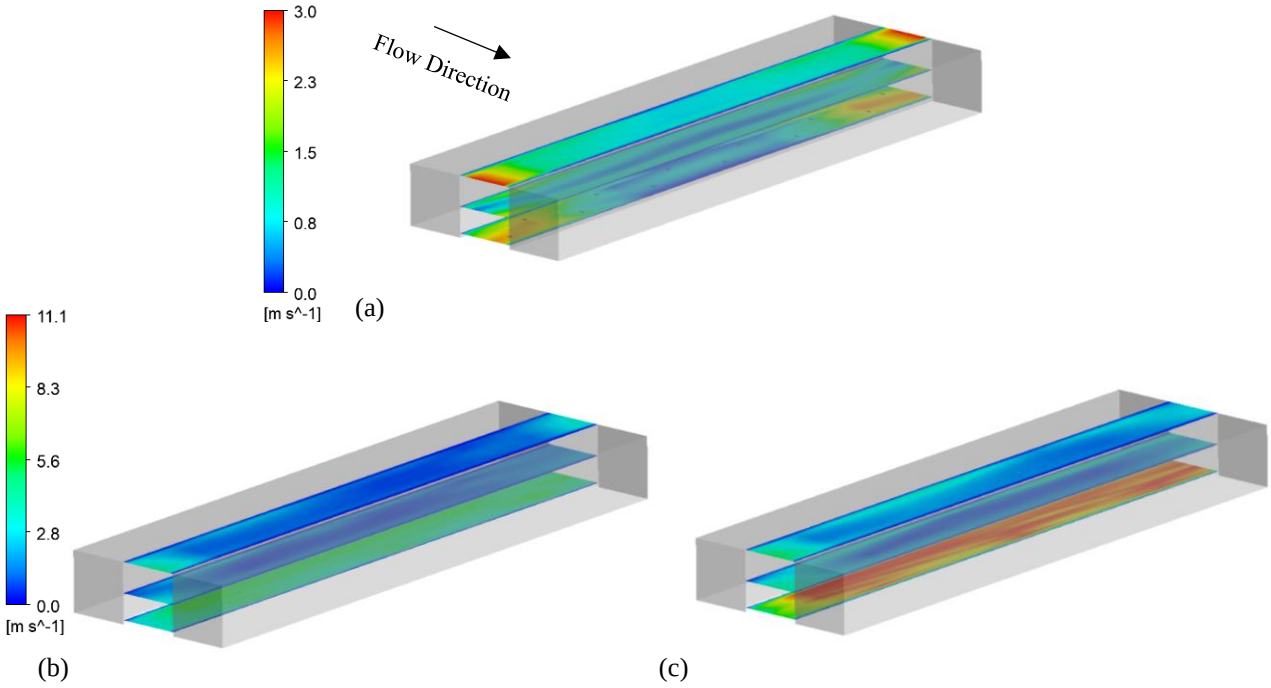

Figure 6. Mean velocity contour at planes z/H = 0.066, z/H = 0.5 e z/H = 1 for vehicle speeds of (a) 0 km/h, (b) 20 km/h and (c) 40 km/h.

Figure 7 shows that the total velocity magnitude increases near the car's regions mainly when they are moving, also, between z/H = 0.5 and z/H = 1 the fluid slows down in all cases due to the buildings wall effects involving the velocity gradient produced and the no slip condition used, possibly contributing to CO accumulation in this region, since there's less turbulent diffusion. From z/H=1 an increase is seen in the velocity for all cases, until it reaches the free stream velocity, where the gradient is small, and the changes are negligible.

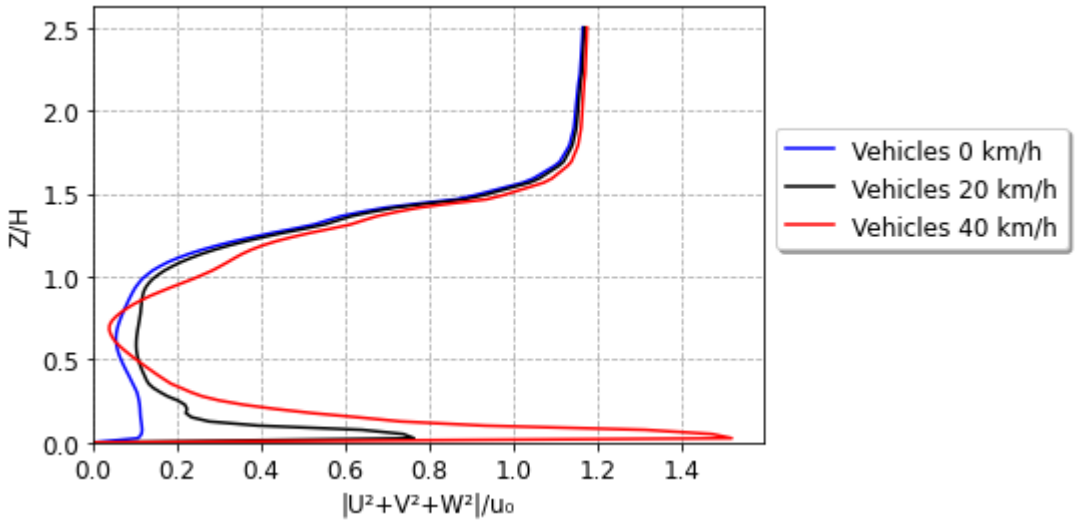

Figure 7. Vertical profile of the averaged 15 vertical lines mean velocity for different vehicle moving speeds.

3.2 Carbon monoxide concentration fields

To validate the CO concentration results a normalized concentration c_* is used as parameter for comparison defined by Equation (10), where $\rho = 1.225\ kg/m^3$ is the air density and c is the concentration obtained from the numerical results. The position of the plane where the concentration contours are analyzed is shown in Figure 8.

$$c_* = \frac{c\rho u_0 H^2}{\dot{m}}. \tag{10}$$

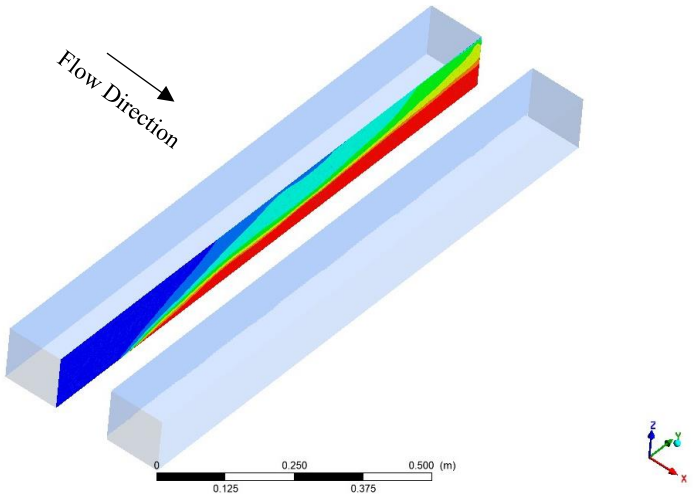

Figure 8. Position of the plane x/H = -0.5 inside the domain.

Figure 9 shows the wind tunnel measurements made by Kastner-Klein et al. (2001) and Figure 10 this paper's numerical results. It is important to note that the validation is made using a case where the vehicle's velocity is 30kmh^{-1}, because that's the velocity that the author used for the wind tunnel experiment.

A comparison between the figures lead to the conclusion that the models used in the numerical simulation could predict the contour pattern and the normalized concentration's order of magnitude, furthermore, an exact match between the results was not expected since Kastner-Klein et al. (2001) used a line source in the experiment to model the cars emission, while this work's used a single CO source in each vehicle, as shown in Figure 2. Given that, the CO concentration results given by the simulation are in reasonable agreement with the wind tunnel data.

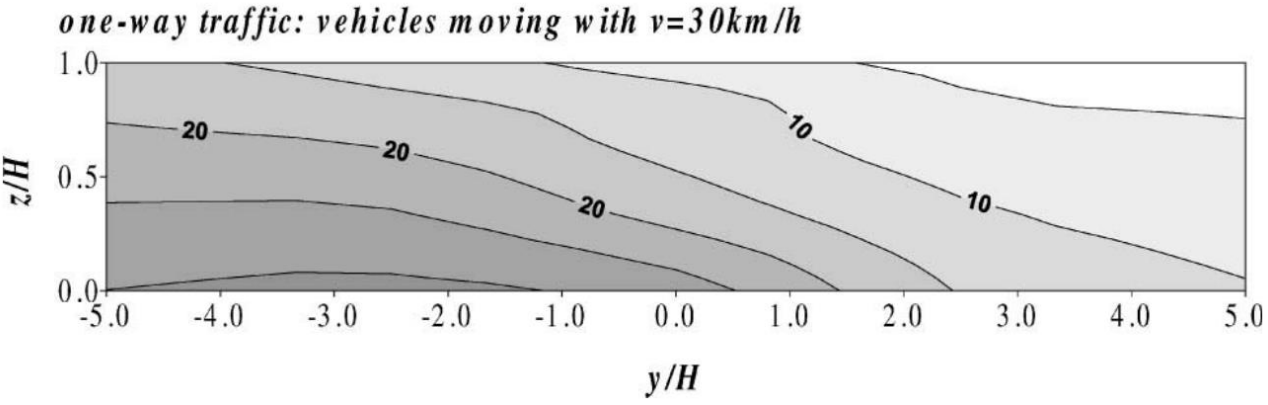

Figure 9. Wind tunnel data of normalized CO concentration contours at the plane x/H = -0.500 for vehicles moving at 30kmh^{-1} (Kastner-Klein et al., 2001).

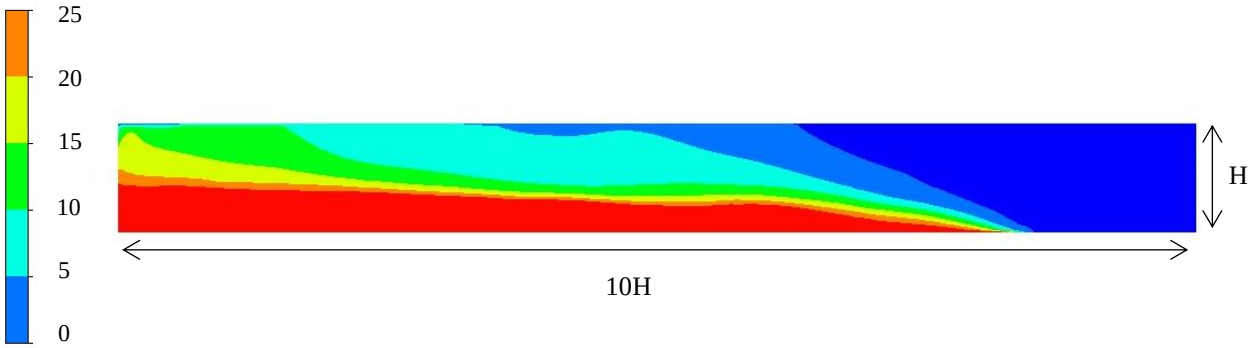

Figure 10. Numerical results of normalized CO concentration contours at the plane x/H = -0.500 for vehicles moving at 30kmh^{-1}.

Analyzing the concentration contours of CO within the canyon, it is noticeable in the Figure 11a the CO accumulation near the floor and next to the upstream building wall, that can be explained by the flow orientation inside the canyon. A big vortex formation favors the transport and accumulation of CO in this region. In that case, the external main flow is perpendicular to the building's length. In Figure 11b the vehicles have a 20kmh^{-1} velocity, and there's a reduction on CO concentration in the planes at half and at the building height. Furthermore, since the pollutant sources are located right behind each vehicle, the plane located at Z/H = 0,066 has high concentrations and the CO is easily carried by the vehicle induced flow. This flow dispersion effect is seen more intensely at Figure 11c, Where the higher planes still have low concentrations and the plane at the vehicle height has less regions with a concentration around 0.1 g/kg, due to the intense convective mass transport, favored by the vehicle velocity increase from 20kmh^{-1} to 40kmh^{-1} . It is also possible to note that the external flow doesn't affect the pollutant dispersion significantly, given that the turbulence induced by the vehicles surpasses the effect of the external flow in this region and is more effective in dispersing the CO, when compared with the standing vehicle case.

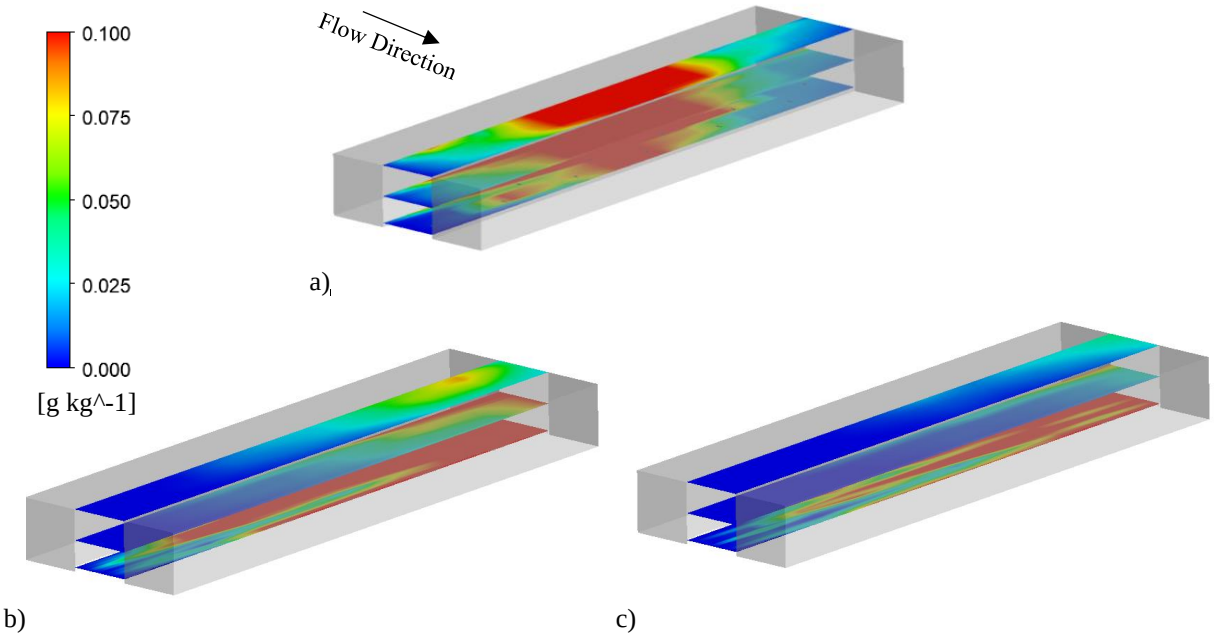

Figure 11. CO concentration contours at planes z/H = 0.066, z/H = 0.5 e z/H = 1 for vehicle speeds of (a) 0 km/h, (b) 20 km/h and (c) 40 km/h.

Figure 12 shows the CO concentration in a vertical line located at the intersection of the planes x/H = 0 and y/H = 0. The concentration values are shown in a logarithmic scale due to the exponential decay nature of it when we move away from the source location. For all cases we see that the concentration is reducing between z/H=0 and z/H=0,5, it increases slightly until z/H=1 and above this height, the main flow effects prevail, generating a continuous and steep reduction of CO concentration. The main factor that differentiates the three curves is that they are horizontally displaced, showing that considering the VIT effects, a 74% mean reduction of CO concentration is obtained, comparing the standing vehicle case

and the 20 kmh^{-1} vehicle case. Also, analyzing the same effect intensity for the 20 kmh^{-1} and 40 kmh^{-1} cases, a mean reduction of 53% is obtained, from the former to the latter.

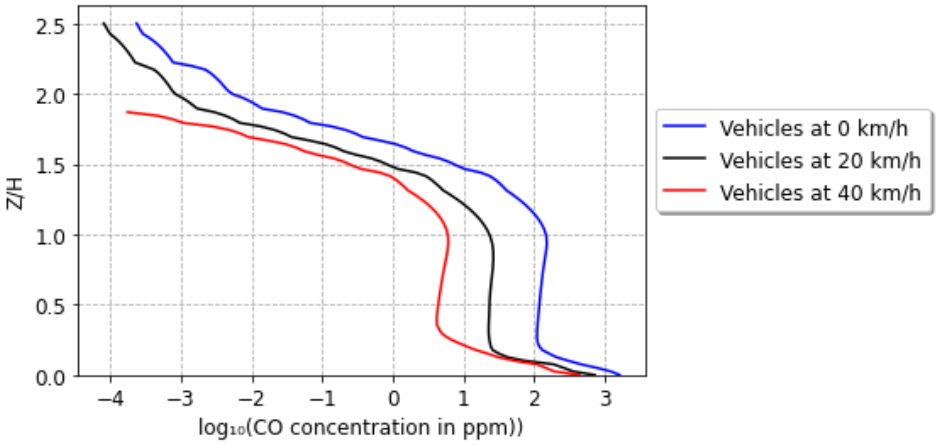

Figure 12. Vertical profiles of CO concentration for different vehicle moving speeds at $x/H = 0$ and $y/H = 0$.

4. CONCLUSIONS

This research showed that numerical approaches to solve pollutant dispersion problems in urban areas are a viable option, given that the adequate models are being used and experimental validations also must take place, ensuring the results reliability. Beyond that, there's still the necessity to study more the dispersion phenomena and search ways of reducing the risks which the world population is exposed.

The modelling through the VIT source term together with the Standard k – ε turbulence closure model showed accuracy, producing similar results to the ones found in literature for both the velocity and CO dispersion analysis, without requiring much computational effort, compared with methods based on dynamic mesh.

The effect of the VIT promotes noticeable changes in the CO transport direction inside the canyon and in its intensity, depending on the speed in which the car is moving. An increase in vehicle speed also increases the turbulent kinetic energy and the turbulent diffusivity, contributing to more intense dispersion and a smaller carbon monoxide concentration. However, these are preliminary results and more effects such as vehicle power usage and the fuel used for combustion should also be analyzed for a better understanding of this problem.

5. ACKNOWLEDGMENTS

We thank IFES campus São Mateus for providing the laboratory and space necessary to develop the research. We also thank FAPES for funding the machines used for this research.

6. REFERENCES

Cai, C. et al. The effect of turbulence induced by different kinds of moving vehicles in street canyons. Sustainable Cities and Society. v. 54. mar. 2020. Available at: http://dx.doi.org/10.1016/j.scs.2020.102015.

CETESB - Companhia Ambiental do Estado de São Paulo. Relatório de Emissões Veiculares no Estado de São Paulo. Governo do Estado de São Paulo. p. 10, 2019.

Kastner-Klein, P.; Fedovorich, E.; Rotach, M. W. A wind tunnel study of organised and turbulent air motions in urban street canyons. Journal of Wind Engineering and Industrial Aerodynamics. v. 89 p. 849-861, 2001.

Oke, T. R. Street Design and Urban Canopy Layer Climate. Energy and Buildings. v. 11. p. 103-113, 1988.

Richards, R.; Hoxey, R., Appropriate boundary conditions for computational wind engineering models using k-epsilon model. Journal of Wind Engineering and Industrial Aerodynamics v. 46, p. 145–153, 1993.

Shi, T. et al. The effect of exhaust emissions from a group of moving vehicles on pollutant dispersion in the street canyons. Building and Environment. v. 181, p. 107-120, 2020.

Solazzo E. et al. Modelling wind flow and vehicle-induced turbulence in urban streets. Atmospheric Environment. v. 42, p. 4918-4931, 2008.

World Health Organization (WHO). Billions of people still breathe unhealthy air: new WHO data. 2022. Available at: https://www.who.int/news/item/04-04-2022-billions-of-people-still-breathe-unhealthy-air-new-who-data. Accessed: 17 jul. 2022.

Zhao et al. Numerical evaluation of turbulence induced by wind and traffic, and its impact on pollutant dispersion in street canyons. Sustainable Cities and Society, v. 74, p. 103-142, 2021.

7. RESPONSIBILITY NOTICE

The authors are the only responsible for the printed material included in this paper.